Hindawi Publishing Corporation
Journal of Ceramics
Volume 2013, Article ID 850751, 7 pages
http://dx.doi.org/10.1155/2013/850751

Research Article

Simple and Rapid Fabrication of $Na_{0.5}K_{0.5}NbO_3$ Thin Films by a Chelate Route

A. Fernández Solarte, N. Pellegri, O. de Sanctis, and M. G. Stachiotti

Laboratorio de Materiales Cerámicos, Universidad Nacional de Rosario, IFIR, CONICET, Avenida Pellegrini 250, S2000BTP Rosario, Argentina

Correspondence should be addressed to N. Pellegri; pellegri@fceia.unr.edu.ar

Received 22 February 2013; Accepted 24 May 2013

Academic Editor: Shaomin Liu

$Na_{0.5}K_{0.5}NbO_3$ (NKN) thin films were prepared by a chelate route which offers the advantage of a simple and rapid solution synthesis. The route is based on the use of acetoin as a chelating agent. The process was optimized by investigating the effects of alkaline volatilization on film properties. While we observed no evidence of stoichiometry problems due to potassium volatilization loss during the heat treatments, thin films synthesized with insufficient sodium excess presented a potassium-rich secondary phase, which has a significant influence on the ferroelectric properties. We show that the amount of spurious phase decreases with increasing Na^+ concentration, in such a way that a 20 mol% Na^+ excess is necessary to fully compensate the volatilization loss that occurred during the heat treatment. In this way, NKN thin films annealed at 650°C presented a well-crystallized perovskite structure, no secondary phases, well-defined ferroelectric hysteresis loops ($P_r \sim 9\,\mu C/cm^2$, $E_C \sim 45\,kV/cm$), and low leakage current density (2×10^{-7} A/cm^2 at 80 kV/cm).

1. Introduction

Lead-free $K_{0.5}Na_{0.5}NbO_3$ (NKN) based ceramics are the most promising candidates for the replacement of lead zirconate titanate (PZT), due to their relatively good piezoelectric properties and high Curie temperature [1]. The miniaturization and integration of devices demand layered structures, which are supported on thin films processing. The fabrication of NKN-based thin films has been investigated by several methods such as pulsed laser deposition (PLD) [2], aerosol-deposited films [3], and mainly by sol-gel techniques [4–6]. Sol-gel techniques are based on the 2-methoxyethanol process. Although this route offers an excellent control and reproducibility of process chemistry, the preparation of the precursor solutions involves distillation and refluxing strategies which makes the solution preparation process difficult.

NKN films produced by chemical solution deposition methods typically have large leakage currents, and it is always difficult to obtain well-saturated polarization hysteresis loops [6]. This drawback comes out from the loss of stoichiometry because Na^+ and K^+ are easy to volatilize during the thermal treatment of the films. The evaporation of the alkali ions produces the appearance of spurious phases and causes the formation of oxygen vacancies in the films that lead to a large leakage current and thus poor ferroelectric and piezoelectric properties. The main strategy for overcoming the problem caused by the loss of alkali ions has been addition an excess of Na^+ and/or K^+ in the initial compositions. How alkaline compositions are lost is an important area of research, including issues such as what the amount of loss is. For example, Tanaka et al. [7] obtained single perovskite phase in 300 nm thick NKN films prepared by sol-gel with the adding of 10 mol% excess of Na^+ in the precursor solution. On the contrary, Kupec et al. [8] used a 5 mol% K^+ excess solution to synthesize 250 nm thick films. Other authors prepared NKN films from precursor solutions with excess of both K^+ and Na^+ [9, 10]. Evidently, there are no identical conclusions in the literature as regards which cation volatilizes more easily, K^+ or Na^+. We note, however, that the results mentioned previously were obtained by using different synthesis parameters, such as thermal sequences, drying, and annealing temperatures, and in some cases different starting materials.

The aim of this work is twofold. Firstly, to develop a chelate route for the synthesis of NKN thin films which

offers the advantage of simple and rapid solution synthesis. In comparison with the 2-methoxyethanol process, distillation and refluxing strategies are not required. Secondly, to optimize the route by investigating the effects of different excess amounts of Na^+ and K^+ in the precursor solutions for the growth of NKN thin films of submicron thickness with good ferroelectric properties. Phase structure and microstructure, ferroelectric *P-E* hysteresis loops, and *J-E* characteristics, as well as the thermal evolution of partner powders, are compared. The influence of the annealing temperature on the ferroelectric properties of the thin films is also investigated.

2. Experimental Procedure

The chelate route relies on the molecular modification of the alkoxide compounds through reactions with other reagents, namely, chelating agents which provide stability to the precursor solutions. Regarding the chelating agent, acetic acid, acetylacetone, or amine compounds are the most commonly used. α-Hydroxyketones, on the other hand, have emerged as good chelating agents due to their stabilization effects on metal alkoxides solutions. In particular, it was found that acetoin (3-hydroxy 2-butanone) has the highest stabilization effect on Ti, Zr, Ta, and Nb metal alkoxides [11, 12]. In the present case, the NKN solutions were prepared starting from sodium ethoxide, potassium ethoxide, and niobium ethoxide as metal precursors, using acetoin and ethanol as chelating agent and solvent, respectively. Firstly, niobium pentaethoxide ($Nb(OCH_2CH_3)_5$, 99.95% Aldrich) was dissolved in a solution of acetoin (3-hydroxy-2butanone, Aldrich) and ethanol with a ratio $[Nb(OCH_2CH_3)_5]/[\text{acetoin}] = 1/4$. Afterwards, one solution of potassium ethoxide ($KOCH_2CH_3$, 24% wt. solution in ethanol, Aldrich) and subsequently another one of sodium ethoxide ($NaOCH_2CH_3$, 21% wt solution in ethanol, Aldrich) were added to the niobium precursor solution. Each step of the procedure was performed under a nitrogen atmosphere and a continuous stirring. The nitrogen atmosphere was maintained during the whole solution preparation process through the use of a controlled atmosphere chamber filled with dry nitrogen. Finally, water (dissolved in ethanol) was added up to reach a molar ratio $[H_2O]/[NKN] = 2$. The NKN molar concentration of the solution was equal to 0.125. Precursor solutions were prepared with a 0 mol% alkaline excess, a 10 and 20 mol% excess amount of sodium ethoxide, and a 15 mol% amount of potassium ethoxide that correspond to the compositions (labeled as): $Na_{0.5}\ K_{0.5}NbO_3$ (NK-0), $Na_{0.55}\ K_{0.5}NbO_3$ (N-10), $Na_{0.6}\ K_{0.5}NbO_3$ (N-20), and $Na_{0.5}K_{0.575}NbO_3$ (K-15), respectively.

To grow the films, the precursor solutions were spin-coated on $Pt/TiO_2/SiO_2/Si$ substrates at 3000 rpm for 30 s in a clean bench. The wet films were dried at 200°C for 7 min. Subsequently, the burning of residual groups in the films was performed at 400°C for 10 min in air. Finally, the samples were annealed in air at temperatures between 600°C and 750°C for 5 min. For thicker films, a multilayer process was used, repeating the coating/heat-treatment cycle three times. The thickness of each sample was determined by ellipsometry using a Rudolph ellipsometer with a wavelength of 634 nm.

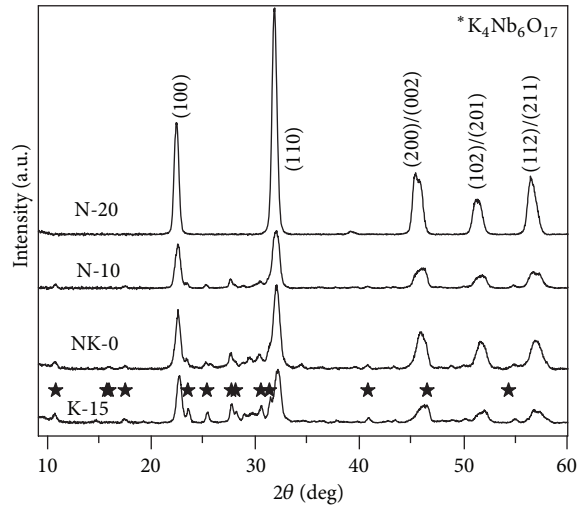

Figure 1: XRD spectra of the powders derived from 20 mol % (N-20), 10 mol% Na^+ excess (N-10), 0 mol% alkaline excess (NK-0), and 15 mol% K^+ excess in precursor solutions (K-15) after annealing at 600°C.

For instance, the thickness of a 0 mol% excess NKN three-layer film annealed at 600°C was 235 ± 3 nm, and its refractive index was 2.074 ± 0.008. As all films were grown in similar conditions, their thicknesses are similar to the previous value.

Gel powders were obtained from the precursor solution by solvent evaporation under a pressure of 40 torr, and, then, the gels were dried at 200°C for 24 h. Thermal analyses (DTA-TG) of the gel powders were performed using a Shimadzu DTG 60H equipment with a heating rate of 10°C/min from room temperature to 600°C in normal atmosphere. Crystal structures of thin films and ceramic powders were analyzed at room temperature using a Philips X'Pert Pro X-ray diffractometer with Cu K_α radiation of wavelength 1.5406 A, at a scan rate of 0.02^0/s. For thin films, the measurements were made with grazing incident X-ray diffraction (GIXRD), using a Soller slit to get parallel beam for diffraction. Surface morphology was observed with scanning electron microscopy using an FE-SEM Philips. To measure the electrical properties of the films, 0.3 mm diameter Pt top electrodes were deposited by DC sputtering on the films and then annealed at 400°C for 60 min. The Pt layer of the substrates was used as bottom electrodes. The dielectric constant and the dielectric loss were measured by complex impedance spectroscopy using an HP 4192 A LF impedances analyzer at frequencies between 1 KHz and 1 MHz. Ferroelectric properties were evaluated using a ferroelectric test system (a conventional Sawyer-Tower circuit) applying AC signals at 1 kHz and at room temperature. The current density (J)-electric field (E) characteristics of the NKN thin films were measured at room temperature using an electrometer/high-resistance meter.

3. Results and Discussions

Figure 1 shows the XRD patterns of partner powders treated at 600°C which are related to each film composition, that is, using 0 mol% alkaline excess, 10 mol%, 20 mol% Na^+, and

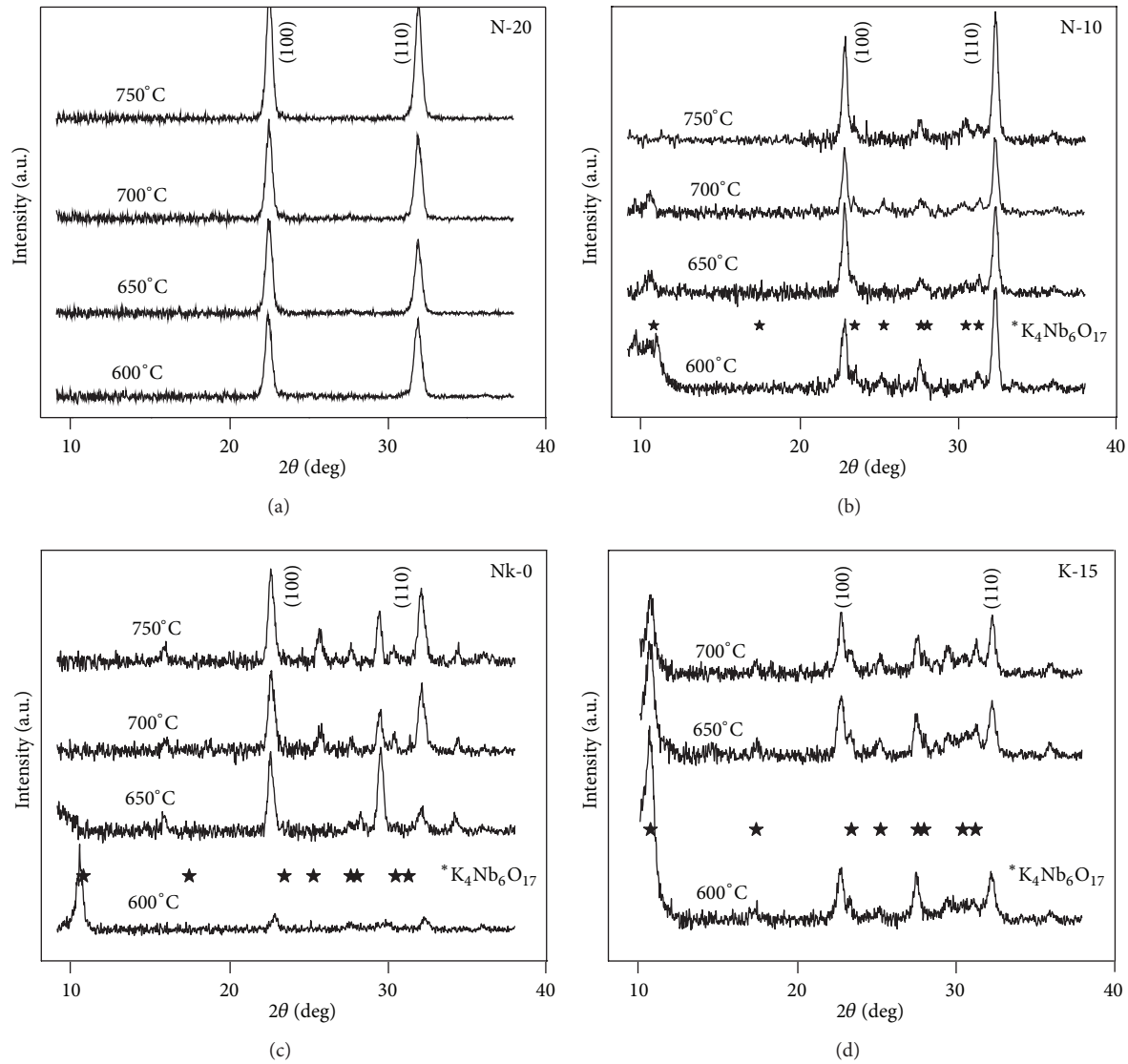

FIGURE 2: XRD spectra of the thin films grown using (a) 20 mol %, (b) 10 mol% Na^+ excess, (c) 0 mol% alkaline excess, and (d) 15 mol% K^+ excess in precursor solutions on $Pt/TiO_2/SiO_2/Si$ substrate after annealing at 600–750°C.

15 mol% K^+ excess precursor solutions, and the names are abbreviated as KN-0, N-10, N-20, and K-15, respectively. We anticipate that the spectra of the thin films are similar to that obtained by the powders. In the case of the powders, however, the peaks corresponding to spurious phases are more intense, clarifying the spectra. While the N-20 powder shows a well-crystallized NKN perovskite as unique phase, the spectrum of the K-15 powder shows additional peaks corresponding to the $K_4Nb_6O_{17}$ tungsten bronze structure, which is the only secondary phase present in the system. It is clear that the increase of the Na^+/K^+ ratio in the precursor solution (see NK-0 and N-10) produces a decrease in the intensity of the peaks corresponding to the spurious phase. Thus, the excess of Na reduces the content of the nonperovskite phase, indicating that the volatilization of Na^+ is more important than K^+ in powders annealed at 600°C.

Figure 2 shows the XRD patterns of the thin films annealed at different temperatures from 600 to 750°C. We show results for 2θ ranged between 10 and 40 degrees in the region where the peaks of the spurious phase are more intensive. All grown films exhibit diffraction peaks corresponding to the NKN perovskite phase. However, only the films derived from the 20 mol% Na^+ excess precursor solution (N-20) (Figure 2(a)) exhibited a spectrum free of spurious phases, with a well-crystallized perovskite structure after being annealed at 600°C. NK-0 thin films annealed at 600°C (Figure 2(c)) showed weak peaks corresponding to the perovskite phase together with $K_4Nb_6O_{17}$ peaks. The intensity of perovskite peaks as well as the one corresponding to spurious phases increase as the annealing temperatures increase. N-10 thin films (Figure 2(b)) developed a better crystallinity; however, their XRD spectra also show nonperovskite peaks although their intensities are much lower than the ones of the NK-0 films. For NKN thin films grown from 15 mol% K^+ excess (Figure 2(d)), the XRD spectra show also peaks corresponding to the spurious phase.

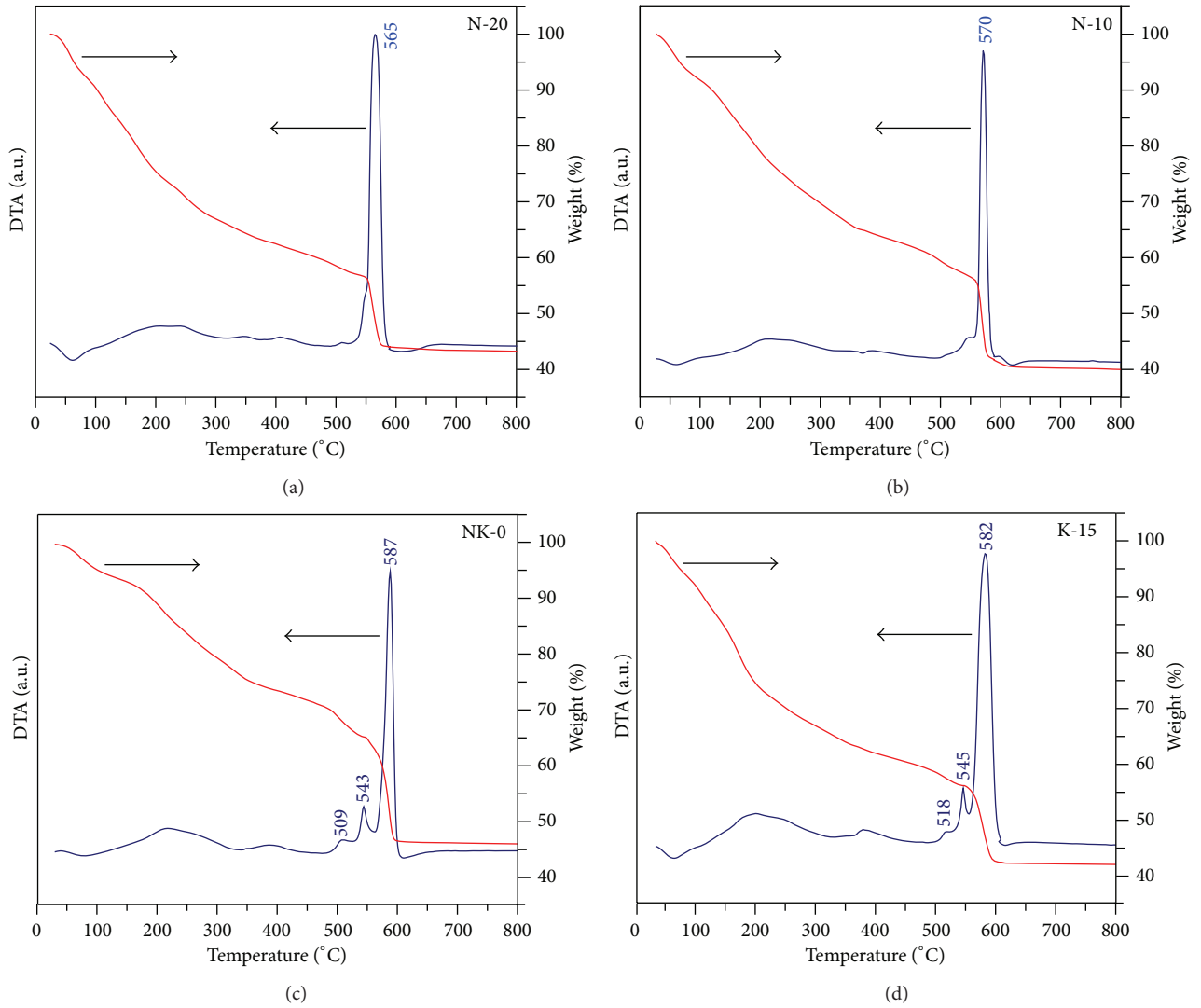

FIGURE 3: DTA-TG curves of the gel powders derived from precursor solutions with (a) 20 mol %, (b) 10 mol% Na^+ excess, (c) 0 mol% alkaline excess, and (d) 15 mol% K^+ excess.

Figure 3 shows the DTA-TG curves of partner powders obtained from precursor solutions after the solvent has been removed. No significant differences between them are observed at temperatures below 450°C. At higher temperatures, the DTA curves of all powders show exothermic peaks centered between 565, and 587°C, coinciding each one with a strong mass loss. Those peaks can be attributed to a massive crystallization of NKN that occurred during the amorphous-crystalline transition. With the increase of Na^+ excess in the precursor solutions, NKN crystallization temperature decreases, the width of the DTA exothermic peak decreases, and the temperature range in which that mass loss occurs is narrower. Other two exothermic peaks are observed in the temperature range between 500°C and 550°C. One is a small peak at around 509°C that tends to disappear when the Na^+ content increases. This peak could be attributed to the crystallization of the $K_4Nb_6O_{17}$ phase, since it is known that the $K_4Nb_6O_{17}$ phase appeared as the first crystalline phase during the heating of the amorphous precursor gel at temperatures around 500°C [13, 14]. The second exothermic peak around 543°C is probably due to the early formation of part of the NKN perovskite phase induced by reaction of the preexisting $K_4Nb_6O_{17}$ phase with the surrounding amorphous material [15]. This peak decreases as the Na content increases and almost disappears for the N-10 sample (Figure 3(b)), and it is completely covered by the peak corresponding to the massive crystallization of NKN in the powder derived from the precursor solution with the highest Na content (Figure 3(a)). Both exothermic peaks at around 509°C and 543°C are accompanied by the loss of mass, whose slope decreases as the Na content increases, indicating that the fraction of amorphous material consumed in each of those reactions decreases with Na^+ content. These results reveal that the increase of Na^+ content in the precursor solutions partially inhibits the early crystallization of the $K_4Nb_6O_{17}$ phase and lowers the crystallization temperature of the NKN perovskite phase, while a Na^+ deficient structure favors the crystallization of the rich potassium phase

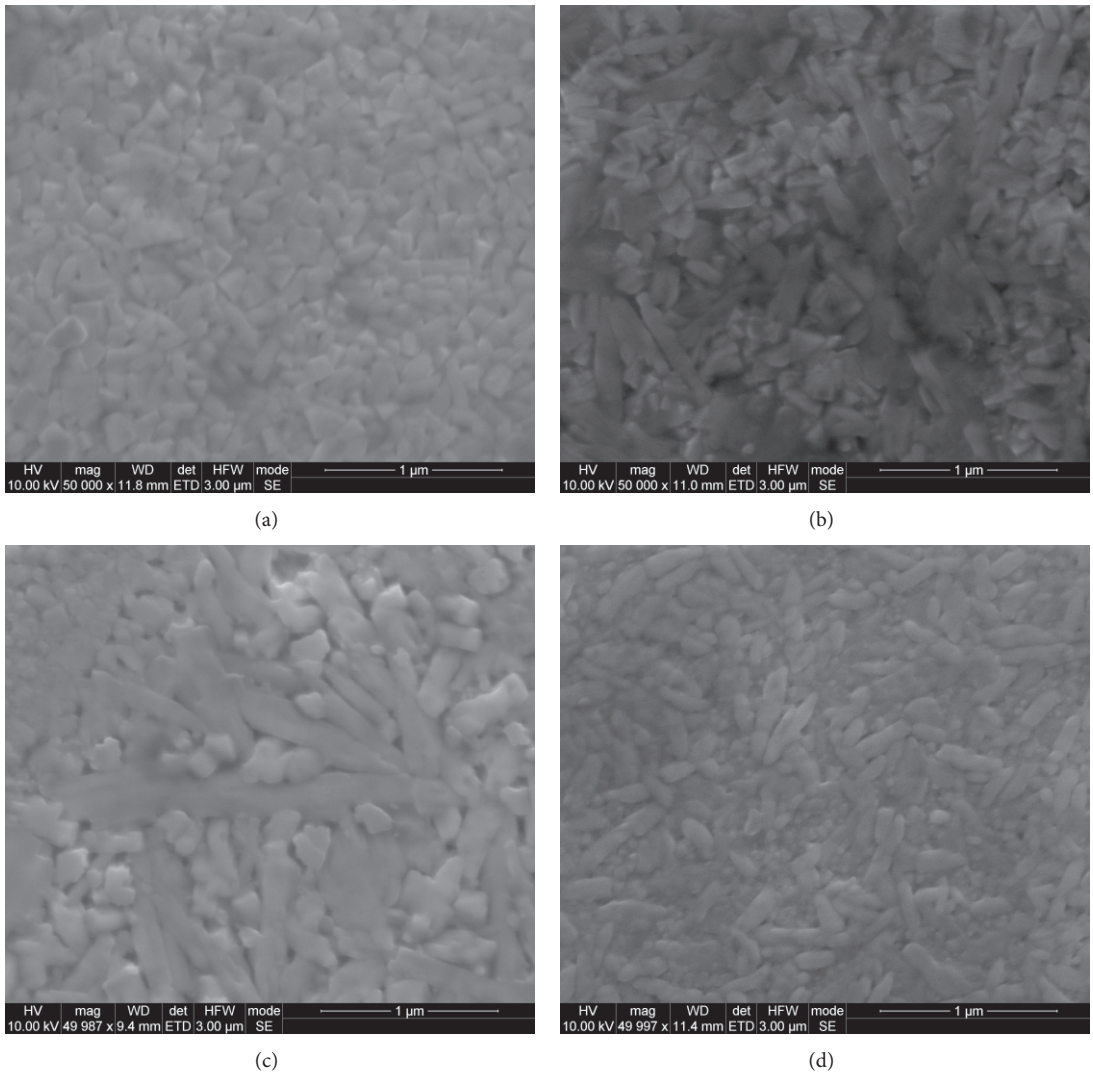

Figure 4: Scanning electron microscopy micrographs of the thin films grown using (a) 20 mol %, (b) 10 mol% Na^+ excess, (c) 0 mol% alkaline excess, and (d) 15 mol% K^+ excess annealed at 650°C.

$K_4Nb_6O_{17}$ [16]. We can thus conclude that a 20 mol% Na^+ excess must be added to the precursor solution to mitigate the Na^+ volatilization. The compensation of the volatilized Na^+ content allows for the achievement of stoichiometry in order to obtain a unique fully crystallized NKN perovskite phase in powder as well as in thin films annealed at 600°C.

Figure 4 shows the microstructure of the NKN thin films that were grown using 0 mol% alkaline excess, 10 mol%, 20 mol% Na^+ excess and 15 mol% K^+ excess, precursor solutions and after being annealed at 650°C, obtained by SEM. Thin films grown with the highest Na^+ content (Figure 4(a)) exhibit a homogeneous and dense microstructure with grains of about 100 nm in size and with almost a single-modal distribution of grain size, indicating a normal grain growth. On the contrary, the microstructure of K-15 thin film is formed by elongated-shaped grains (Figure 4(d)). NK-0 and N-10 films present polycrystalline microstructures that consist of two different grain types. We can observe in Figures 4(b) and 4(c) the presence of highly anisotropic grains immersed into a fine-grained dense material. This highly anisotropic grain growth can be related to the fact that the crystallization of these grains does not occur directly from the amorphous precursor but through an asymmetric intermediate crystalline phase; that is, during the heating of the Na-deficient amorphous films, this asymmetric phase is the first to be formed.

Figure 5 shows the *P-E* hysteresis loops for NK-0, N-10, N-20, and K-15 thin films annealed at 650°C. The measurements were conducted at a switching frequency of 50 Hz and a maximum applied field of 150 kV/cm. The NK-0 and K-15 thin films almost do not display ferroelectric behavior, while the N-10 thin film exhibited a very slim ferroelectric hysteresis loop. Only the film grown from the 20 mol% Na^+ excess precursor solution exhibited a well-saturated hysteresis loop, with a relatively high remnant polarization of $P_r = 8.2\,\mu C/cm^2$ and a coercive field of $E_C = 55$ kV/cm. Moreover, the N-20 thin films tolerate a very high applied electric field, over 300 kV/cm. Figure 6 shows the *P-E*

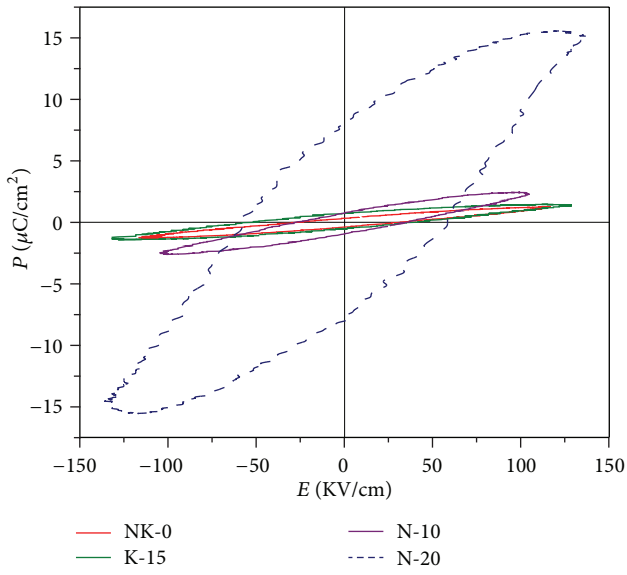

FIGURE 5: Ferroelectric *P-E* hysteresis loops for NKN thin films grown using 20 mol % (N-20), 10 mol% Na^+ excess (N-10), 0 mol% alkaline excess (NK-0), and 15 mol% K^+ excess (K-15) in precursor solutions on $Pt/TiO_2/SiO_2/Si$ substrate after annealing at 650°C.

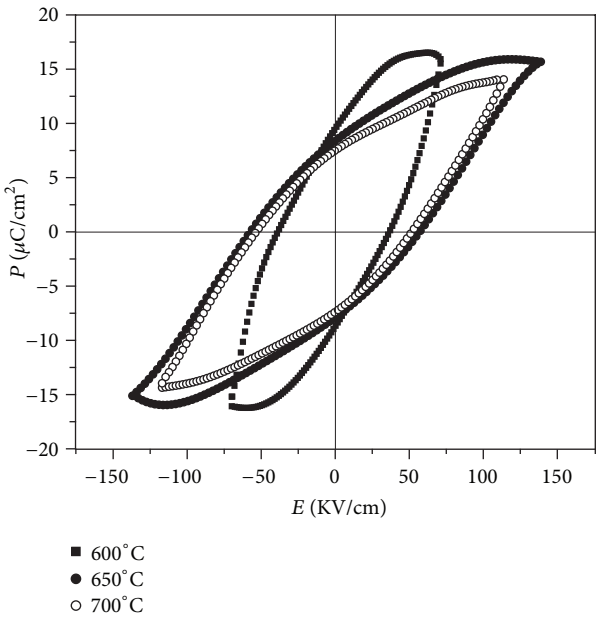

FIGURE 6: The *P-E* hysteresis loops of the 20%mol Na^+ excess NKN thin films after annealing at 600°C (■), 650°C (●), and 700°C (○).

ferroelectric hysteresis loops for N-20 thin films annealed at 600, 650 and 700°C. All films show typical ferroelectric behavior. Remnant polarizations of 10, 8.2, and 7.5 $\mu C/cm^2$ and the coercive fields of 33, 45, and 55 kV/cm were obtained for the films annealed at 600, 650, and 700°C, respectively. Although the film annealed at 600°C presents the highest P_r and the lowest E_C, its hysteresis loop is rounded in shape, indicating large leakage components. The films annealed

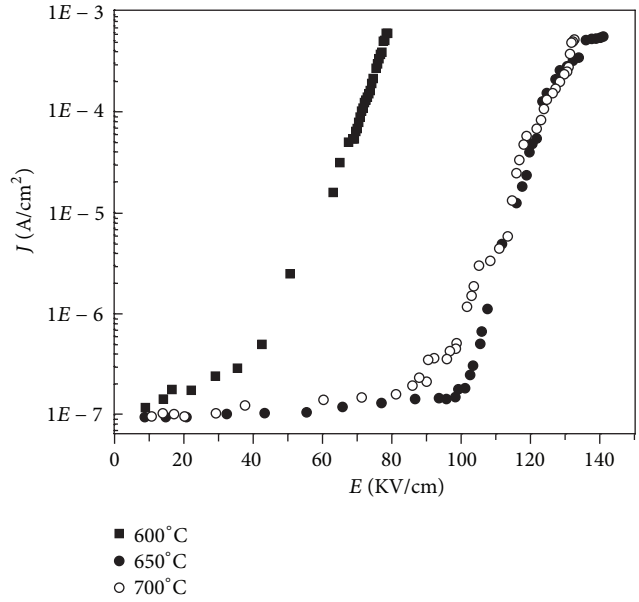

FIGURE 7: *J-E* curves of 20%mol Na excess$^+$ NKN thin films after annealing at 600°C (■), 650°C (●), and 700°C (○).

at higher temperatures exhibited better ferroelectric loops. Figure 7 shows room-temperature *J-E*characteristics of the N-20 films annealed at 600, 650, and 700°C. The leakage current densities were around 10^{-7} A/cm^2 at electric fields lower than 30 kV/cm. For electric fields ranged between 40 and 80 kV/cm, the leakage current density of the film annealed at 600°C rapidly increased from 10^{-6} to 10^{-3} A/cm^2. On the contrary, the leakage current densities of the films annealed at 650 and 700°C remain lower than 2×10^{-7} A/cm^2 for electric fields up to 100 kV/cm. Once this value is achieved, the leakage current increases abruptly.

The leaky ferroelectric *P-E* hysteresis loops as well as the high-leakage current at low field of the N-20 thin film annealed at 600°C would be caused by residual defects. The amorphous gel-crystalline transition left residual defects of synthesis, such as dangling bonds and "noncharge compensation vacancies of oxygen" [17, 18]. These defects remain in the film structure until the diffusion mechanism becomes an operative process, which allows the oxygen absorption into the structure and consequently produces structural healing and annihilation of the oxygen vacancies that occurs at a temperature range between 600 and 650°C [19]. "Noncharge compensation vacancies" are missing atoms that behave as neutral vacancies when the structure has crystallized. Neutral oxygen vacancies act as donor defects. First ionization, $V_O^x \rightarrow V_O^\bullet + e^-$, has a very low ionization energy ($\Delta h <$ 0.2 eV); on the contrary, the ionization energy is higher for double ionization: $V_O^x \rightarrow V_O^{\bullet\bullet} + 2e^- (\Delta h < 1.5\,\text{eV})$ [20]. First-ionization vacancy would be responsible for the high-leakage current at low field and the leaky hysteresis loop display in the N-20 thin film annealed at 600°C. The incorporation of oxygen in the structure produces the annihilation of oxygen vacancies, but the annihilation of the "noncharge

compensation vacancies" does not produce electrical carriers, $(1/2)O_2 + V_O^x \rightarrow (1/2)O_2 + V_O^{\bullet} + e^- \rightarrow O_O$.

4. Conclusions

We developed a chelate route for the synthesis of NKN thin films using acetoin as a chelating agent. The route offers the advantage of a simple and rapid solution synthesis; in comparison with the 2-methoxyethanol method, distillation and refluxing strategies are not required. The process was optimized by investigating the effects of alkaline volatilization on film properties. While no evidence of stoichiometry problems was detected due to potassium volatilization loss, the volatility of Na^+ complicates the growth of phase-pure films. Na-deficient compositions favor an early crystallization of a $K_4Nb_6O_{17}$ secondary phase. We showed that the addition of a 20 mol% Na^+ excess to the NKN precursor solution was effective in compensating for the volatilization of Na at moderate temperatures, lowering at the same time the crystallization temperature of the perovskite phase. In this way, NKN films annealed at 650°C present a well-crystallized perovskite structure, good ferroelectric properties, and low leakage current.

Conflict of Interests

The authors declare no conflict of interests regarding commercial entities mentioned in this paper.

Acknowledgments

The authors wish to acknowledge financial support from Consejo Nacional de Investigaciones Científicas y Técnicas (CONICET) and Universidad Nacional de Rosario. M. G. Stachiotti thanks CIUNR support.

References

[1] Y. Saito, H. Takao, T. Tani et al., "Lead-free piezoceramics," *Nature*, vol. 432, no. 7013, pp. 84–87, 2004.

[2] T. Saito, T. Wada, H. Adachi, and I. Kanno, "Pulsed laser deposition of high-quality (K,Na)NbO_3 thin films on $SrTiO_3$ substrate using high-density ceramic targets," *Japanese Journal of Applied Physics B*, vol. 43, no. 9, pp. 6627–6631, 2004.

[3] J. Ryu, J.-J. Choi, B.-D. Hahn, D.-S. Park, W.-H. Yoon, and K.-H. Kim, "Fabrication and ferroelectric properties of highly dense lead-free piezoelectric $(K_{0.5}Na_{0.5})NbO_3$ thick films by aerosol deposition," *Applied Physics Letters*, vol. 90, no. 15, Article ID 152901, 2007.

[4] F. Lai and J.-F. Li, "Sol-gel processing of lead-free (Na,K)NbO_3 ferroelectric films," *Journal of Sol-Gel Science and Technology*, vol. 42, no. 3, pp. 287–292, 2007.

[5] K. Tanaka, K.-I. Kakimoto, and H. Ohsato, "Fabrication of highly oriented lead-free (Na, K)NbO_3 thin films at low temperature by Sol-Gel process," *Journal of Crystal Growth*, vol. 294, no. 2, pp. 209–213, 2006.

[6] Y. Nakashima, W. Sakamoto, H. Maiwa, T. Shimura, and T. Yogo, "Lead-free piezoelectric (K,Na)NbO_3 thin films derived from metal alkoxide precursors," *Japanese Journal of Applied Physics*, vol. 46, no. 12–16, pp. L311–L313, 2007.

[7] K. Tanaka, H. Hayashi, K.-I. Kakimoto, H. Ohsato, and T. Iijima, "Effect of (Na,K)-excess precursor solutions on alkoxy-derived (Na,K)NbO_3 powders and thin films," *Japanese Journal of Applied Physics B*, vol. 46, no. 10, pp. 6964–6970, 2007.

[8] A. Kupec, B. Malic, J. Tellier, E. Tchernychova, S. Glinsek, and M. Kosec, "Lead-free ferroelectric potassium sodium niobate thin films from solution: composition and structure," *Journal of the American Ceramic Society*, vol. 95, no. 2, pp. 515–523, 2012.

[9] Y. Nakashima, W. Sakamoto, T. Shimura, and T. Yogo, "Chemical processing and characterization of ferroelectric (K,Na)NbO_3 thin films," *Japanese Journal of Applied Physics B*, vol. 46, no. 10, pp. 6971–6975, 2007.

[10] C. W. Ahn, S. Y. Lee, H. J. Lee et al., "The effect of K and Na excess on the ferroelectric and piezoelectric properties of $K_{0.5}Na_{0.5}NbO_3$ thin films," *Journal of Physics D*, vol. 42, no. 21, Article ID 215304, 2009.

[11] T. Ohya, M. Kabata, T. Ban, Y. Ohya, and Y. Takahashi, "Effect of α-hydroxyketones as chelate ligands on dip-coating of zirconia thin films," *Journal of Sol-Gel Science and Technology*, vol. 25, no. 1, pp. 43–50, 2002.

[12] Y. Takahashi, A. Ohsugi, T. Arafuka, T. Ohya, T. Ban, and Y. Ohya, "Development of new modifiers for titanium alkoxide-based sol-gel process," *Journal of Sol-Gel Science and Technology*, vol. 17, no. 3, pp. 227–238, 2000.

[13] K. Tanaka, K.-I. Kakimoto, H. Ohsato, and T. Iijima, "Effects of Pt bottom electrode layers and thermal process on crystallinity of alkoxy-derived (Na,K)NbO_3 thin films," *Japanese Journal of Applied Physics A*, vol. 46, no. 3, pp. 1094–1099, 2007.

[14] K. Tanaka, K.-I. Kakimoto, and H. Ohsato, "Morphology and crystallinity of $KNbO_3$-based nano powder fabricated by sol-gel process," *Journal of the European Ceramic Society*, vol. 27, no. 13–15, pp. 3591–3595, 2007.

[15] I. Pribošič, D. Makovec, and M. Drofenik, "Formation of nanoneedles and nanoplatelets of $KNbO_3$ perovskite during templated crystallization of the precursor gel," *Chemistry of Materials*, vol. 17, no. 11, pp. 2953–2958, 2005.

[16] L. Y. Wang, K. Yao, P. C. Goh, and W. Ren, "Volatilization of alkali ions and effects of molecular weight of polyvinylpyrrolidone introduced in solution-derived ferroelectric $K_{0.5}Na_{0.5}NbO_3$ films," *Journal of Materials Research*, vol. 24, no. 12, pp. 3516–3522, 2009.

[17] R. Caruso, E. Benavídez, O. de Sanctis et al., "Phase structure and thermal evolution in coating films and powders obtained by sol-gel process: part II. ZrO_2 -2.5 mole % Y_2O_3," *Journal of Materials Research*, vol. 12, no. 10, pp. 2594–2601, 1997.

[18] M. C. Caracoche, P. C. Rivas, M. M. Cervera et al., "Zirconium oxide structure prepared by the sol-gel route: I, the role of the alcoholic solvent," *Journal of the American Ceramic Society*, vol. 83, no. 2, pp. 377–384, 2000.

[19] M. G. Stachiotti, R. MacHado, A. Frattini, N. Pellegri, and O. de Sanctis, "Effects of the chemical modifier on the thermal evolution of $SrBi_2Ta_2O_9$ precursor powders," *Journal of Sol-Gel Science and Technology*, vol. 36, no. 1, pp. 53–60, 2005.

[20] I. Tanaka, F. Oba, K. Tatsumi, M. Kunisu, M. Nakano, and H. Adachi, "Theoretical formation energy of oxygen-vacancies in oxides," *Materials Transactions*, vol. 43, no. 7, pp. 1426–1429, 2002.